

MAGNETIC DESIGN OF QUADRUPOLES FOR THE MEDIUM AND HIGH ENERGY BEAM TRANSPORT LINE OF THE LIPAC ACCELERATOR*

C. Oliver[#], B. Brañas, A. Ibarra, I. Podadera, F. Toral, CIEMAT, Madrid, Spain

Abstract

The LIPAC accelerator will be a 9 MeV, 125 mA cw deuteron accelerator which will verify the validity of the design of the future IFMIF accelerator. A Medium Energy Beam Transport line (MEBT) is necessary to handle the high current beam from the RFQ to the Superconducting RF accelerating cavities (SRF) whereas a High Energy Beam Transport line (HEBT) is used to match the beam from the SRF to the beam dump. The high space charge and beam power determine the beam dynamics in both transport lines. As a consequence, magnets with strong fields in a reduced space are required. Along the transport beamlines, there are different types of quadrupoles with steerers and a dipole. Special care is devoted to maximize the integrated fields in the available space. Both 2-D and 3-D magnetic calculations are used to optimize coil configurations. Magnetic performance and cost, both of magnet and power supply, have been taken into account for final choice. In this paper, the design of the resistive quadrupoles of the MEBT and HEBT of the LIPAC accelerator is presented.

INTRODUCTION

In order to test materials for future fusion energy reactors, the International Fusion Materials Irradiation Facility (IFMIF) will provide an accelerator-based D-Li high energy neutron source [1]. To demonstrate the high current operation of the accelerator and validate the design of its components, a 9 MeV, 125 mA cw deuteron accelerator (LIPAC) is being designed [2]. It consists of an injection section, an RFQ, a Medium Energy Beam Transport (MEBT) line [3], a superconducting linac based on half wave resonator cavities and a High Energy Beam Transport (HEBT) line. In the transport lines there are located different resistive quadrupoles (five in the MEBT and eight in the HEBT) to keep the high current ion beam focused, whereas a bending magnet is used to drive the beam to the beam dump. Additionally pairs of horizontal/vertical dipole correctors (four in the MEBT and six in the HEBT) are included to correct the beam centre deviations.

RESISTIVE QUADRUPOLE REQUIREMENTS FOR LIPAC

The main magnet parameters like aperture, integrated magnetic field and required field quality are determined by beam optics considerations. However, in order to simplify the design and construction and minimize the cost, it is proposed to reduce the different types of

quadrupoles to four, whose main requirements are summarized in Table 1.

Table 1: Quadrupole and steerer specifications

Type	A	B	C	D	Units
Location	MEBT	HEBT 1 st triplet	HEBT Doublet	HEBT 2 nd triplet	-
Quad gradient	25.0	14.5	8.0	12.75	T/m
Aperture	56	90	136	136	mm
Integrated field (75% aperture)	0.068	0.081	0.061	0.163	T.m
Steerers	25	30	30	30	G.m

Concerning the field quality, the amplitude of multipole components should be $<10^{-3}$ at 75% of the mechanical aperture. Additional limitations come from the small available longitudinal space for these magnets in the accelerator.

QUADRUPOLE AND STEERER CONFIGURATION

Separate steering magnets (commonly used due to their good field quality) can not be considered in our case due to space restrictions. After studying different possibilities [4] the final choice has been adding independent dipole windings to the quadrupole to produce the required steerer field in both horizontal and vertical planes. An schematic representation of quadrupole and steerer coils and iron in 2D is shown in Fig. 1.

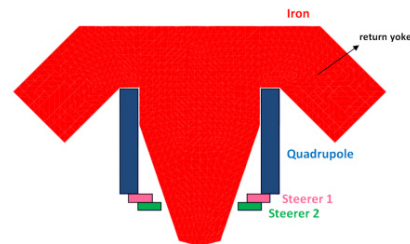


Figure 1: Schematic representation of quadrupole and steerer coils around the iron pole.

High-conductivity oxygen-free copper OF-OKTM conductors with a round hole for water cooling (hollow conductors) have been used for the quadrupole coil design. Concerning the steerers, air-cooled ETP (Electrolytic Tough Pitch) copper conductors have been chosen due to their low dissipated power.

Inter-turn insulation made of a layer of E-type half-lapped epoxy impregnated fiberglass tape with a 0.25 mm

* Work partially supported by Spanish Ministry of Science and Innovation under project AIC10-A-000441 and ENE2009-11230.

[#]concepcion.oliver@ciemat.es

thickness for quadrupoles and 0.125 mm for steerers have been considered in our design. Additionally 1.5 mm (0.5 mm) ground insulation must be placed around the whole quadrupole (steerer) coil.

The quadrupole coil geometry has been carefully chosen to reduce the longitudinal length of the quadrupole but also to minimize the transversal magnet size and, therefore, the cost. In the case of the quadrupole type D, the high iron saturation has motivated the use of cone-shaped coils as a better choice to reduce the saturation whereas planar coils have been considered for the rest of quadrupoles.

The steerer coils have been designed as double pancakes and have been located below the quadrupole coils in order to take advantage of the available space close to the pole tip.

Concerning the iron, due to its high saturation field, the ARMCO steel has been selected for our design. More details about iron profile optimization are shown elsewhere [4].

MAGNETIC CALCULATIONS

Electromagnetic simulations of the quadrupole field have been performed using the CERN field computation code ROXIE [6]. Due to the short length of the MEBT and HEBT quadrupoles, the field is dominated by end effects and therefore 3D optimizations have been performed to obtain the required integrated gradient with low content of harmonics ($<10^{-3}$) and saturation.

The required number of Ampere-Turns has been determined by electromagnetic simulations, especially in the case of steerers, due to the high quadrupole-steerer coupling. Taking into account the effect of the current density on the power loss and the magnet size and keeping in mind the reduced available space for magnets in the transport lines of LIPAC accelerator, current densities about 5-6 A/mm² for quadrupoles has been considered.

The results of the magnetic computations when only quadrupole coils are energized at maximum NI are summarized in Table 2. Integrated harmonics are shown for a radius equal to 75% of the aperture.

Table 2: Quadrupole Integrated Field Quality

Quad Type	A	B	C	D	Units
Integrated field	0.070	0.085	0.066	0.169	T.m
b_6/b_2	0.230	0.059	0.029	0.144	10^{-4}
b_{10}/b_2	0.443	1.145	0.921	0.275	10^{-4}
b_{14}/b_2	2.646	3.090	4.46	3.128	10^{-4}

The gradient uniformity (integrated in z) is below 0.05% for all quadrupole types. Figure 2 shows the quadrupole uniformity for the type A. Black line represents the region inside 75% of quadrupole aperture.

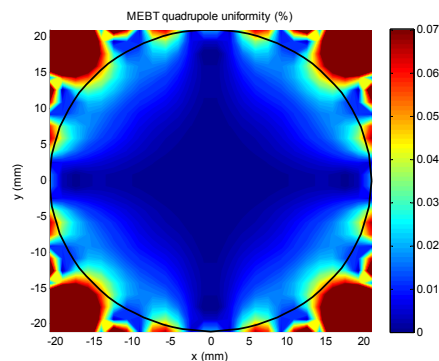


Figure 2: Gradient uniformity for type A magnet.

The quadrupole saturation dependence on the excitation current has been studied for the different magnet types. Figure 3 depicts that the magnet behaviour is linear up to 70-80% of the nominal current, showing non-linearity for higher currents. It is observed that for the quadrupole type D, even using cone-shaped coils, the saturation is the highest. However, the saturation of that quadrupole type would even be about 40% higher at maximum current in the case of planar coils.

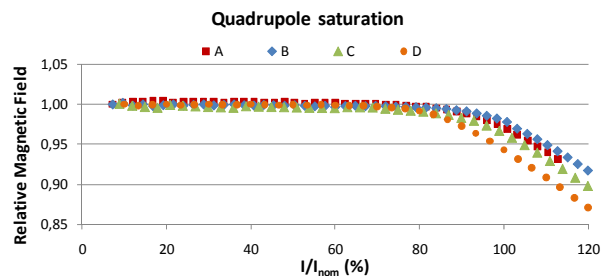


Figure 3: Transfer function.

It should be remarked that quadrupoles will usually operate at lower gradients than the maximum design gradient, reducing strongly the saturation during normal operation (lower than 0.5% for all quadrupoles).

Quad-quad Coupling

Since the proximity between adjacent quadrupoles will lead to a non-negligible interaction, a combined model with the contiguous quadrupoles has been studied. Figure 4 shows the magnetic field for the separate quadrupoles and the combined model for the type B magnet (nominal gradients given by beam dynamics simulations have been used). The difference at the center of each magnet is small (lower than 1%) for all quadrupole types.

Steerers

Magnetic simulations of steerers show a high contribution of the sextupole component (about 35% of the dipole field), which is due to the surrounding quadrupole yoke. Higher harmonics are lower than 2%. Although the steerer field quality is not very good, beam

dynamics simulations have shown no appreciable deterioration of the beam transport.

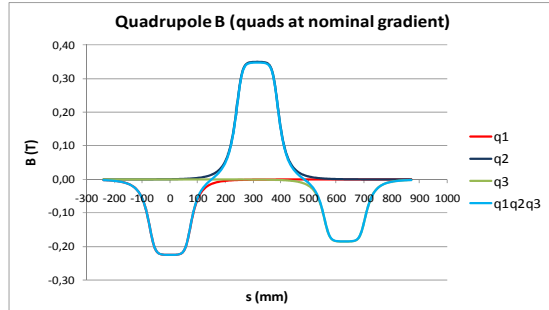


Figure 4: Quadrupole coupling for type B magnet

Quad-steerer Coupling

Another consequence of the steerer configuration is the strong quadrupole-steerer coupling. Fig. 5 shows the evolution of the steerer field at maximum current when quadrupole is powered at different currents. Although the quad-steerer coupling is high at full quadrupole current (35% in the case of the most saturated quadrupole), quadrupole gradients during operation will be much lower, leading to negligible saturation and consequently very small quad-steerer coupling (lower than 2%).

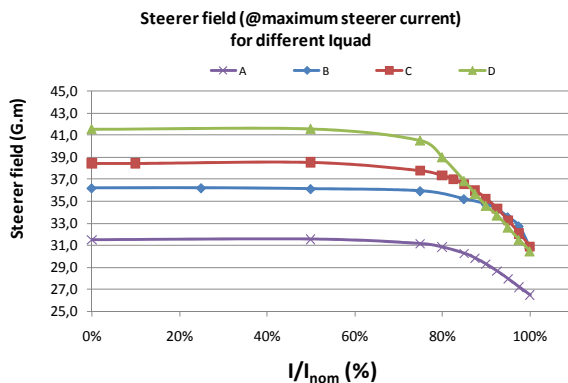


Figure 5: Steerer field for different quadrupole currents.

ELECTRIC AND COOLING CALCULATIONS

For the quadrupole water cooling, typical assumptions for resistive magnets have been taken into account in our design [5]. Concerning the steerers, the current density has been limited to values about 2 A/mm^2 due to the air cooling choice. A summary of the main magnet parameters are shown in Table 3.

CONCLUSIONS

Space restrictions in the LIPAC accelerator have strongly influenced the design of the resistive magnets of the transport lines, leading to a compact solution where the steerer field is obtained with additional coils in the quadrupole yoke. The magnet field quality has been accepted from the beam dynamics point of view and the

coupling between adjacent magnets will be small during normal operation.

Table 3: Quadrupole and Steerer Parameters

Type	A	B	C	D	Units
NI_{quad}	7850	11690	14700	23475	A.Turns
I_{quad}	178.4	229.2	257.9	313.0	A
j_{quad}	5.9	5.0	5.7	5.4	A/mm^2
P_{quad}	2.0	3.3	5.0	11.6	kW
R_{quad}	61.9	62.0	75.0	118.0	$\text{m}\Omega$
V_{quad}	11.0	14.2	19.4	37.1	V
ΔP	5.0	5.0	5.0	5.0	bar
v	1.7	1.5	1.4	1.3	m/s
Water flow rate	3.0	3.6	3.2	8.5	l/min
ΔT	9.4	13.1	22.4	19.5	$^{\circ}\text{C}$
NI_{steerer}	400	570	950	630	A.Turns
I_{steerer}	22.2	20.4	29.7	16.6	A
j_{steerer}	2.2	2.0	2.1	1.7	A/mm^2
P_{steerer}	33.1	55.5	103.0	75.7	W
R_{steerer}	67.0	134.0	117.0	275.0	$\text{m}\Omega$
V_{steerer}	1.5	2.7	3.5	4.5	V
Assembly Length	180.0	213.0	181.0	332.0	mm
Assembly Weight	0.15	0.39	0.47	1.50	Ton

REFERENCES

- [1] IFMIF Comprehensive Design Report, IFMIF International Team, January 2004.
- [2] A. Mosnier et al., "The Accelerator Prototype of the IFMIF-EVEDA Project", IPAC'10, Kyoto (2010).
- [3] I. Podadera et al., "The Medium Energy Beam Transport line of LIPAC", IPAC'11, these proceedings.
- [4] I. Podadera et al., "Preliminary Design Review: MEBT Definition Report", LIPAC Internal Note, BA_D_22QS7F v1.1, January 2010.
- [5] J. Tanabe, "Iron Dominated Electromagnets Design, Fabrication, Assembly and Measurements", SLAC-R-754, June 2005.
- [6] S. Russenschuck, "Roxie: A computer for the integrated design of accelerator magnets", CERN, LHC-Project-Report-276, 1999.